



UNIVERSITY OF LEEDS

This is a repository copy of *NMR Self Diffusion and Relaxation Time Measurements for Poly (vinylidene fluoride) (PVDF) Based Polymer Gel Electrolytes Containing LiBF<sub>4</sub> and Propylene Carbonate*.

White Rose Research Online URL for this paper:  
<http://eprints.whiterose.ac.uk/100044/>

Version: Accepted Version

---

**Article:**

Richardson, PM, Voice, AM and Ward, IM (2016) NMR Self Diffusion and Relaxation Time Measurements for Poly (vinylidene fluoride) (PVDF) Based Polymer Gel Electrolytes Containing LiBF<sub>4</sub> and Propylene Carbonate. *Polymer*, 97. pp. 69-79. ISSN 0032-3861

<https://doi.org/10.1016/j.polymer.2016.03.074>

---

© 2016, Published by Elsevier. Licensed under the Creative Commons Attribution-NonCommercial-NoDerivatives 4.0 International  
<http://creativecommons.org/licenses/by-nc-nd/4.0/>

**Reuse**

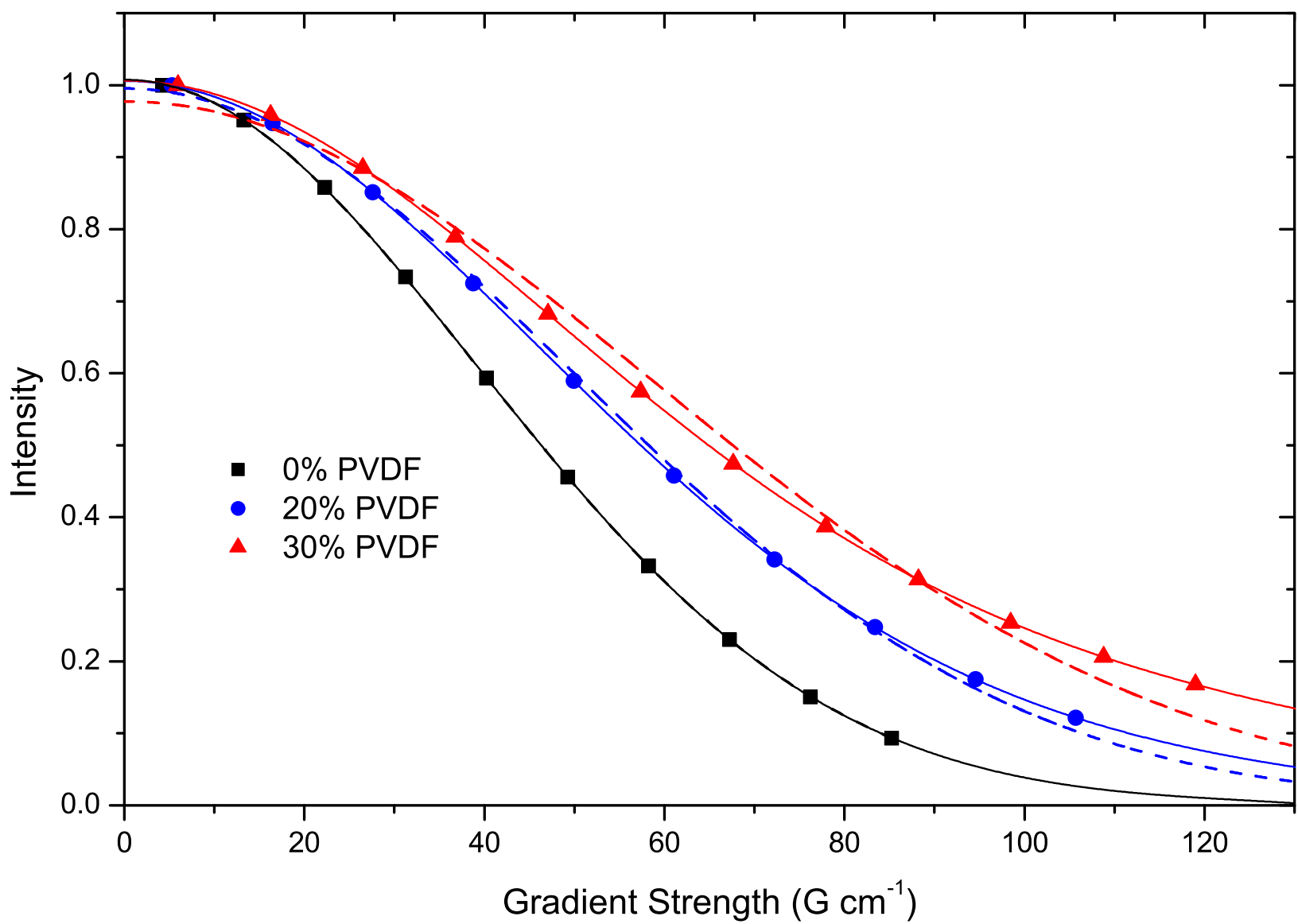
Items deposited in White Rose Research Online are protected by copyright, with all rights reserved unless indicated otherwise. They may be downloaded and/or printed for private study, or other acts as permitted by national copyright laws. The publisher or other rights holders may allow further reproduction and re-use of the full text version. This is indicated by the licence information on the White Rose Research Online record for the item.

**Takedown**

If you consider content in White Rose Research Online to be in breach of UK law, please notify us by emailing [eprints@whiterose.ac.uk](mailto:eprints@whiterose.ac.uk) including the URL of the record and the reason for the withdrawal request.



[eprints@whiterose.ac.uk](mailto:eprints@whiterose.ac.uk)  
<https://eprints.whiterose.ac.uk/>



# NMR Self Diffusion and Relaxation Time Measurements for Poly (vinylidene fluoride) (PVDF) Based Polymer Gel Electrolytes Containing $LiBF_4$ and Propylene Carbonate

P.M. Richardson, A.M. Voice, I.M. Ward\*

*Soft Matter Physics, School of Physics and Astronomy, University of Leeds, Leeds, LS2 9JT, UK*

---

## Abstract

Polymer gel electrolytes (PGEs) have been prepared using lithium tetrafluoroborate ( $LiBF_4$ ), propylene carbonate (PC) and poly (vinylidene fluoride) (PVDF). Self diffusion coefficients have been measured using pulse field gradient nuclear magnetic resonance (PFG-NMR) for the lithium cation,  $BF_4$  anion and solvent molecules using  $^7Li$ ,  $^{19}F$  and  $^1H$  nuclei, respectively. It was found that lithium ion diffusion was slow compared to the much larger fluorinated  $BF_4$  anion, which is attributed to a large solvation shell around the lithium ions. The  $^7Li$  and  $^1H$  diffusion measurements also exhibited two unique environments for the diffusive species. The measurement of NMR transverse relaxation times has confirmed the presence of lithium ions in multiple phases as shown by the diffusion measurements.

*Keywords:* NMR, diffusion, polymer gel electrolyte,  $LiBF_4$ , transverse relaxation, PVDF

---

## 1. Introduction

Polymer gel electrolytes (PGEs) are membranes which consist of a polymer, an organic solvent and a salt. Polymer electrolytes are the focus of much research due to their primary application of use in electrochemical devices and more specifically secondary lithium batteries. The first instance of conductive polymers for use as possible electrochemical devices were presented in research carried out by Armand[1, 2] and Wright[3, 4].

---

\*Corresponding Author

*Email addresses:* [p.m.richardson87@gmail.com](mailto:p.m.richardson87@gmail.com) (P.M. Richardson), [a.m.voice@leeds.ac.uk](mailto:a.m.voice@leeds.ac.uk) (A.M. Voice), [i.m.ward@leeds.ac.uk](mailto:i.m.ward@leeds.ac.uk) (I.M. Ward)

*Preprint submitted to Elsevier*

*23rd February 2016*

Since this early research into solid polymer electrolytes there has been significant research, which has resulted in the evolution of dry polymer electrolytes to polymer gel electrolytes which contain high levels of organic solvent, this evolution is detailed in several reviews of polymer electrolytes [5, 6, 7, 8]. The introduction of an organic solvent increased ion mobility and thus ionic conductivity. These gels are considered important as they offer many properties that traditional lithium ion batteries do not exhibit, such as enhanced safety features (since polymer gel electrolyte batteries do not contain free liquid outside the polymer structure). PGEs are also highly flexible and versatile and are easily produced. Due to easy fabrication by an extrusion lamination method, patented at the University of Leeds, there is no need for external casing or a polymer separator used to stop electrodes shorting [9].

Conducting polymer electrolyte research at the University of Leeds was initiated by Bannister et al [10], who showed that through the use of amorphous comb shaped polymers relatively high conductivities could be achieved, these comb shaped polymers consisted of methacrylate backbones and short poly(ethylene glycol) side chains and teeth [11]. The next approach explored at Leeds consisted of producing gel electrolytes from poly (N,N dimethylacrylamide) (PDMA), conductivities of around  $10^{-4}$  S cm<sup>-1</sup> were obtained at room temperature [12]. These high conductivities were achieved with lithium salts and including the incorporation of N,N dimethylacetamide (DMAc) as a plasticiser [12]. The promising conductivities values achieved here led to a major research programme exploring thermoreversible polymer gel electrolytes based on poly(vinylidene fluoride) (PVDF) for use in advanced secondary battery applications [13].

In this paper we describe thermo-reversible gels produced from PVDF, this was chosen as the host polymer due to it being chemically inert and stable under 4V; which is required for battery applications. PVDF is a polar polymer and thus has a relatively high dielectric constant, which aids in ionic dissociation of the salt ions and therefore increases ionic conductivity. PVDF is a semi crystalline polymer, which forms non chemically cross linked junctions, allowing the resulting polymer gel electrolytes to be thermo-reversible. The semi crystalline gels form crystalline junctions within the solution below the melting temperature. The crystalline junctions will enter a melt if the melting temperature is exceeded due to the absence of chemical cross-links. These distinct properties of

PVDF have resulted in many publications on PGEs containing PVDF, as both the host polymer [13, 14, 15, 16, 17, 18] and as part of co-polymer systems (such as PVDF-HFP)[19, 20, 21, 22].

Research into solid polymer electrolytes by Armand[1, 2] and Wright[3, 4] using poly(ethylene oxide) (PEO) mixed with various lithium based salts, resulted in very low conductivities ( $\approx 10^{-5}$ ). It was found that within these solid polymer electrolytes the ions located in the amorphous regions of the polymer were responsible for the conductivity[4]. In order to enhance the conductivity in the polymer gel electrolytes the location of the ions and the conduction mechanism must be understood. It is therefore the aim of this paper to address the location of the anion and cation within the gel structure.

The precise structure of the polymer gel electrolytes is dependent on many contributing factors. However, the gels are usually found to be formed from aggregations of spherulites, which are believed to contain highly ordered crystalline lamellae which are connected by amorphous polymer to form spherical structures. It has been found that the size and shape of the spherulites are highly dependent on the rate of cooling once the gel has been formed [23]. A paper by Shimizu *et al* [24] shows via SEM that gels produced using diethyl carbonate (DEC) produces rough edged spherulites, where as  $\gamma$ -butyrolactone (GBL) and propylene carbonate (PC) both produce smooth edged spherulites. Although the term spherulite is commonly used in the literature regarding the gelation process, it is not clear the means by which these spherulites are formed. It has been suggested by Chou *et al* that the gelation is a four step process; nucleation and growth into spherical structures, aggregation of the spherical structures, diffusion controlled coarsening and finally Ostwald ripening [25]. Chou *et al* [26] have suggested that the spherulites may not be crystalline and instead the structure of the gels consists of an aggregation of non crystalline spherulitic structure, however it has been observed by Voice *et al* [13] at the University of Leeds that there are clearly crystalline regions within the polymer gel structure.

Since the primary application of these polymer gel electrolytes is for use in secondary lithium batteries, it is important to understand the location of the ions within the gels.  $T_{1\rho}$  measurements carried out by Hubbard *et al* [27] showed that PVDF based polymer gel electrolytes contain multiple phases including a crystalline lamellae phase, an inter-

lamellae amorphous polymer phase, a solvated amorphous polymer phase and a pure liquid phase. These phases were determined by using NMR relaxation times using the hydrogen ( $^1\text{H}$ ) nucleus which will therefore have detected the polymer and the solvent molecules[27]. However, it is important to understand the role of the salt ions as these are responsible for conduction. In this paper we discuss the possibility of the lithium ions being present in multiple phases of the gels and in a subsequent publication will link these results with conductivity data in order to show that there are likely at least two conduction mediums for the lithium ions[28].

In this paper we have used NMR self diffusion measurements to understand the mobility of the solvent molecules, lithium cations and  $\text{BF}_4$  anions using  $^1\text{H}$ ,  $^7\text{Li}$  and  $^{19}\text{F}$  resonant frequencies, respectively. NMR diffusion measurements have been proven to be a useful tool in understanding the mobility in polymer gel electrolytes [29, 30, 31, 32, 16, 33, 34]. However, the possibility of multiple diffusive species of both the lithium ions and solvent molecules is discussed in this paper, which has previously been reported by us [18] and also in a publication by Magistris *et al* [17]. However, this paper will contain a more in depth observation of the NMR diffusion as a function of salt concentration, polymer concentration and temperature.

## 2. Experimental Methods

### 2.1. PGE Preparation

All samples were prepared in an oxygen-free nitrogen filled glove box, in order to reduce the moisture content within the sample. The liquid electrolytes were prepared by mixing  $\text{LiBF}_4$  (lithium tetrafluoroborate) salt with propylene carbonate (PC) at different concentrations. The PVDF polymer was then added to the liquid mixture and heated to 433K (160°C). The weight percentage of polymer to solvent used was 0%wt (liquid electrolyte), 20%wt and 30%wt PVDF. The thermo-reversible gels were produced under high temperature (433 K) and stirring and allowed to cool at ambient temperature. The 99.7% anhydrous propylene carbonate and  $\text{LiBF}_4$  from Sigma-Aldrich were used as received. The Solef  $\text{\textcircled{R}}$ 1015 PVDF used was supplied by Solvay chemicals and placed in the dry glove box before use.

## 2.2. NMR Diffusion

The diffusion coefficients were measured using a 400 MHz Bruker AVANCE II NMR spectrometer. The NMR pulse sequence used was a complex bipolar stimulated echo pulse field gradient (BPStE-PFG) originally designed by Cotts [35]. The Cotts sequence is an adapted from the Stejskal-Tanner pulse sequence [36] which eliminates background magnetic fields. Background magnetic field gradients manifest due to inhomogeneities in the magnetic field. This produces cross terms of the applied magnetic gradients and the background magnetic gradients. This introduces the relation for intensity of signal in the form of equation 1.

$$I = I_1 \exp \left( -D_1 (2\pi\gamma\delta G)^2 \left( \Delta - \frac{\delta}{3} \right) \right) \quad (1)$$

where  $G$  is the gradient field strength,  $\Delta$  is the time between subsequent gradient pulses and  $\delta$  is the gradient pulse duration. The introduction of bipolar pulses resolves the problem of the background magnetic field and allows measurement of the self diffusion coefficients. Bipolar pulses are two gradient pulses of equal magnitude with opposite sign.

The different nuclei were isolated by applying radio frequency pulses corresponding to the resonant frequency of the nuclei. The duration of the  $\pi/2$  pulses were 18.5  $\mu\text{s}$  and 19.6  $\mu\text{s}$  at a power level of 3 dB for  $^7\text{Li}$  and  $^{19}\text{F}$ , respectively. The NMR parameters used were  $\Delta = 40$  ms,  $\delta = 10$  ms. These values were used as they have been proven to work with this type of measurement elsewhere [37].

## 2.3. Transverse Relaxation Times

The transverse relaxation times were measured on a Bruker 400 MHz AVANCE II Ultrashield NMR spectrometer for the  $^7\text{Li}$   $^{19}\text{F}$  measurements and a 50 MHz Maran bench top NMR spectrometer for the  $^1\text{H}$  measurements. The  $\pi/2$  pulses were set as 18.5  $\mu\text{s}$  and 19.6  $\mu\text{s}$  at a power level of 3 dB for  $^7\text{Li}$  and  $^{19}\text{F}$ , respectively. The bench top NMR spectrometer was only capable of measuring using the  $^1\text{H}$  resonant frequency, the pulse duration was set as 3.5  $\mu\text{s}$ .

Both spectrometers used 10 mm diameter glass tubes. Due to the viscous nature of the resulting polymer gel electrolytes, the samples were placed inside the glass tubes

while in the molten state (above 433K). The gels were created and sealed inside the tube while inside the oxygen free glove box, this was to ensure no moisture or impurities were introduced to the sample.

The transverse relaxation times ( $T_2$ ) were measured using the Carr-Purcell-Meiboom-Gill (CPMG) pulse sequence [38] on both NMR spectrometers. The CPMG sequence is an extension of a simple Hahn echo sequence [39]. This pulse sequence involves applying a  $\pi/2$  excitation pulse, after time  $\tau$  the spins will have lost coherence and can be recovered using a spin echo. The echo pulse ( $\pi$ ) is applied after time  $\tau$ , then after another  $\tau$  interval the spins will be realigned causing a spin echo. The CPMG sequence only records every second spin echo, this is to reduce the effect of an imperfect pulse sequence. The CPMG pulse sequence takes the form;

$$\frac{\pi}{2} - [\tau - \pi - \tau]_n \quad (2)$$

where  $\pi/2$  and  $\pi$  refers to the 90° and 180° pulses, respectively,  $\tau$  is an arbitrary time and  $n$  is an integer that must be even for the CPMG pulse sequence.

The sequence was iterated with varying values of  $\tau$ , the decay of the intensity as a function of time takes the form;

$$M_{xy}(t) = M_0 \exp\left[\frac{-t}{T_2}\right] \quad (3)$$

where  $M_{xy}(t)$  is the magnetisation in the xy plane as a function of time,  $M_0$  is the magnetisation in the xy plane immediately after the initial excitation pulse,  $t$  is the time after the initial pulse and  $T_2$  is the transverse relaxation time. When measuring using the Bruker AVANCE II the sequence records the number of spin echoes which have been performed rather than the time taken. Therefore in order to use equation 3 the number of spin echoes must be converted into time, the time taken can be determined in terms of the pulse durations;

$$t = \tau_{\pi/2} + n_{echo}(2\tau + \tau_{\pi}) \quad (4)$$

where  $\tau_{\pi/2}$  and  $\tau_{\pi}$  are the durations of the  $\pi/2$  and  $\pi$  pulses, respectively and  $n_{echo}$  is the number of spin echoes which have been applied. The values of  $\tau$  used had to be determined for each sample, as if the value of  $\tau$  is too long then the magnetisation will fully decay before the measurement has been carried out.



### 3. Results

#### 3.1. NMR Self Diffusion

The self diffusion coefficients for the solvent, anion and cation were measured independently using hydrogen ( $^1\text{H}$ ), lithium ( $^7\text{Li}$ ) and fluorine ( $^{19}\text{F}$ ) resonant frequencies, respectively. The  $^1\text{H}$  resonant frequency was used to measure the diffusion of the PC molecules, however will also detect the polymer; as will the  $^{19}\text{F}$  resonant frequency. Since the polymer is not as mobile as the solvent and ion molecules, the polymer signal will not affect the diffusion measurement. Therefore it can be assumed that the signal from the  $^1\text{H}$  and  $^{19}\text{F}$  measurements are therefore attributed to the solvent and  $\text{BF}_4$  ions in solution, respectively. It should be noted that although there are different formations and clusters of the ions and solvent molecules within the solution, they will be indistinguishable with NMR unless the timescales of the diffusive species are very different, the values obtained are therefore an ensemble average.

It has been previously concluded via  $T_{1\rho}$  in research carried out at the University of Leeds that there are several distinct phases within the PVDF polymer gel electrolytes, including; a crystalline lamellae polymer phase, an inter-lamellae polymer phase, a solvated amorphous polymer phase and a pure liquid electrolyte phase [27]. It is important to understand where the ions are located in the structure, as this will directly affect the ionic conductivity of the gels.

Figure 1 displays the diffusion intensity decay curve as a function of gradient strength ( $G$ ) for 0% (liquid electrolyte), 20% and 30% PVDF/ PC/  $\text{LiBF}_4$  (1.0M) polymer gel electrolytes at 293 K. An interesting feature of the lithium diffusion measurements for the gels was that the data could not be fitted with a single exponential in the form of equation 1, suggesting that the decay in the intensity was caused by multiple distinct diffusive species. Two diffusive regions has been previously reported by this group for PVDF based gels[18] and also elsewhere using PVDF-HFP as the host polymer [17].

The data displayed in figure 1 was fitted with equation 3 (dashed line) which was insufficient to fit the data for the polymer gel electrolytes. All of the data in figure 1 was also fitted with an additional exponential term (solid line) in series of the form;

$$I = I_1 \exp\left(-D_1 (2\pi\gamma\delta G)^2 \left(\Delta - \frac{\delta}{3}\right)\right) + I_2 \exp\left(-D_2 (2\pi\gamma\delta G)^2 \left(\Delta - \frac{\delta}{3}\right)\right) \quad (5)$$

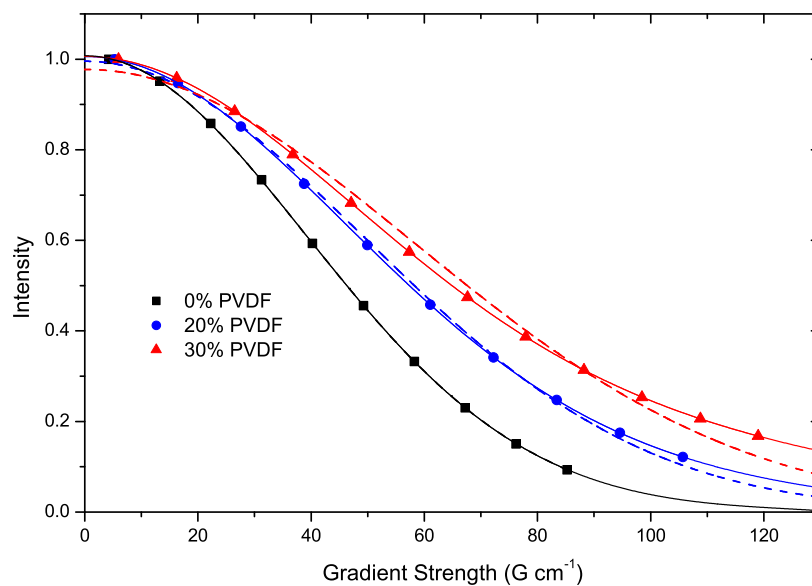


Figure 1: Intensity decay profile for  ${}^7\text{Li}$  NMR self diffusion measurements for 0% (liquid electrolyte), 20% and 30% PVDF/ PC/  $\text{LiBF}_4$  (1.0 M) polymer gel electrolytes at 293 K. The data in each case has been fitted with equation 1 (dashed line) and 5 (solid line), which represents a single and two diffusive species, respectively.

PVDF wt.	Diffusion ( $\times 10^{-10} \text{ m}^2 \text{ s}^{-1}$ )			Intensity (%)	
	$D_1$	$D_2$	$D_{liquid}$	$I_1$	$I_2$
20	0.27	0.67	0.86	28	72
30	0.17	0.66	0.86	37	63

Table 1:  $^7\text{Li}$  diffusion constant fitting parameters for 20% and 30% PVDF/ PC/  $\text{LiBF}_4$  polymer gel electrolytes shown in figure 1.

where  $I_1$  and  $I_2$  are the intensities of the fitting and  $D_1$  and  $D_2$  are the diffusion constants of the two diffusive species. In figure 1 it can be noted that for the liquid electrolyte data the single exponential (equation 1) and double exponential (equation 5) perfectly overlap suggesting a single diffusive species. As previously mentioned the liquid electrolyte will contain different arrangements of the lithium ion, i.e. lithium solvated by PC molecules and lithium ions associated with  $\text{BF}_4$  anions. Therefore the single diffusion coefficient obtained for the liquid here is an ensemble average over all arrangements. The single exponential shown in figure 1 is clearly insufficient for the gels. However, the introduction of a second exponential term (solid line) greatly increased the fit. Unlike in the liquid electrolytes, the lithium ions in the polymer gel electrolytes seem to be located within two distinct environments.

All of the fitting parameters from figure 1 are summarised in table 1. The diffusion constants obtained from figure 1 for the 20% PVDF/ PC/  $\text{LiBF}_4$  (1.0M) were 0.27 and 0.67 ( $10^{-10} \text{ m}^2 \text{ s}^{-1}$ ) with corresponding intensity values of 28% and 72%, respectively. The faster diffusing species is also the more dominant signal for the intensity decay. Since the value of the slower diffusive species is of the same order of magnitude the signals likely originate from two different phases, both with relatively low viscosity. Both of these phases are relatively mobile and therefore suggests that the faster of the two phases is linked with the pure liquid electrolyte phase and the slower of the two is the solvated amorphous phase [27]. Magistris et al [17] observed two possible phases, which they attributed to the liquid and solvated amorphous polymer phase within their polymer gel electrolytes based on PVDF-HFP. The diffusion values for the 30% PVDF/ PC/  $\text{LiBF}_4$  (1.0M) polymer gel electrolyte from figure 1 were 0.17 and 0.66 ( $10^{-10} \text{ m}^2 \text{ s}^{-1}$ ) with corresponding intensity values of 37% and 63%, respectively.

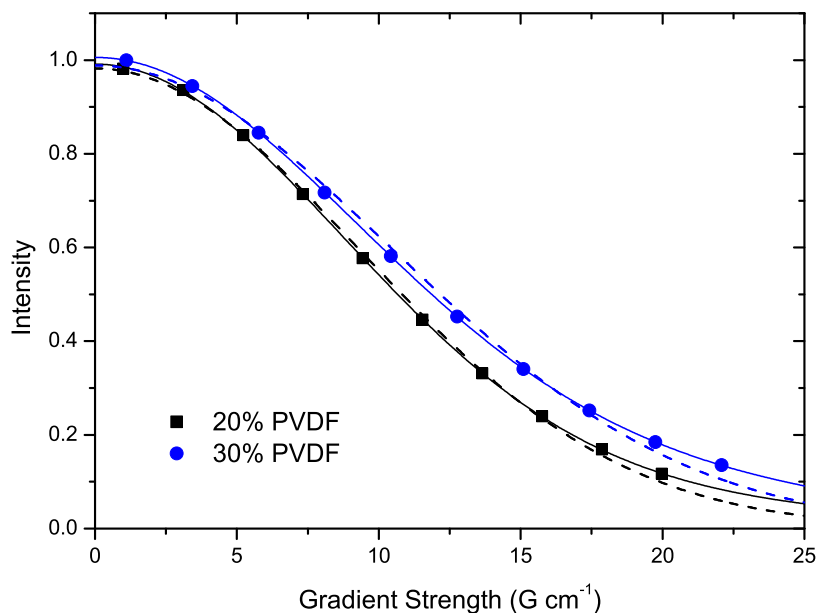


Figure 2: Intensity decay profile for  $^1\text{H}$  NMR self diffusion measurements for 20% and 30% PVDF/ PC/  $\text{LiBF}_4$  (0.5 M) polymer gel electrolytes at 303 K. The data in each case has been fitted with equation 1 (dashed line) and 5 (solid line), which represents a single and two diffusive species, respectively.

With the introduction of more polymer the intensity of the slower phase has increased from 28% up to 37%, which is reasonable if the slower phase is indeed the solvated polymer phase, as this would cause an increase the amount polymer in the system. The faster diffusion (liquid electrolyte phase) value for the two gels were very similar, suggesting that the viscosity liquid electrolyte phase remains approximately constant, however the proportion of the liquid phase has been reduced.

Figure 2 shows the intensity decay curve for the diffusion of 20% and 30% PVDF/ PC/  $\text{LiBF}_4$  using the  $^1\text{H}$  resonant frequency at 303 K, the fitting parameters are summarised in table 2. As previously stated, since the diffusion of the solvent molecules is orders of magnitude greater than the gyration of the polymer, a contribution from the polymer will not be observed. The hydrogen measurements have also been fitted with equations 1 and 5, to represent a single (dashed line) and two exponential fit (solid line), respectively. Much like the lithium measurements shown in figure 1, it can be noted that the hydrogen decay curve also requires a second exponential term. The diffusion values obtained from

PVDF wt.%	Diffusion ( $\times 10^{-10} \text{ m}^2 \text{ s}^{-1}$ )			Intensity (%)	
	$D_1$	$D_2$	$D_{liquid}$	$I_1$	$I_2$
20	0.64	2.59	4.10	13	87
30	0.83	2.55	4.10	31	69

Table 2:  $^1\text{H}$  diffusion constant fitting parameters for 20% and 30% PVDF/ PC/  $\text{LiBF}_4$  (0.5M) polymer gel electrolytes shown in figure 2.

figure 2 for the 20% PVDF gel are 0.64 and 2.59 ( $10^{-10} \text{ m}^2 \text{ s}^{-1}$ ) with corresponding intensity values of 13% and 87%, respectively. The diffusion values obtained for the 30% PVDF gel were 0.83 and 2.55 ( $10^{-10} \text{ m}^2 \text{ s}^{-1}$ ) with corresponding intensity values of 31% and 69%, respectively. As with the lithium measurements, the introduction of more polymer into the system increased the intensity of the slower (solvated amorphous PVDF) phase. The value of the diffusion for the liquid phase are very similar in each gel suggesting again that the amount of polymer does not effect the viscosity of the solution but rather the contribution of each phase.

Unlike the lithium measurements, the two phases determined via the diffusion constant measurements were not as easily detected for the 20% PVDF gels, as they were in the 30% PVDF gel electrolytes. It is likely that there is solvent within the two phases of the gels since there are clearly lithium ions present in both phases. The difficulty in distinguishing the solvent molecules in the two phases within the gel likely arises either due to lower concentration of solvent molecules located in the secondary phase due to the lower polymer concentration or that the diffusion constant values of the two phases are similar. By observing the intensity of the solvated amorphous phase of the lithium and hydrogen measurements, it can be noted that the solvated amorphous phase contained a greater ratio of lithium: solvent molecules than in the liquid phase, however it is presumed that the lithium ions are still fully solvated in the amorphous phase.

The fluorine ( $^{19}\text{F}$ ) diffusion intensity decay curve can be seen in figure 3 for the liquid electrolyte and 30% PVDF/ PC/  $\text{LiBF}_4$  (1.0M) at 303 K. Unlike the other two nuclei investigated here, the  $^{19}\text{F}$  measurements did not display two clear distinct phases. The inset of figure 3 is present to highlight that the two fitting procedures do not perfectly overlap and there is therefore some indication that the  $\text{BF}_4$  anions are present in both

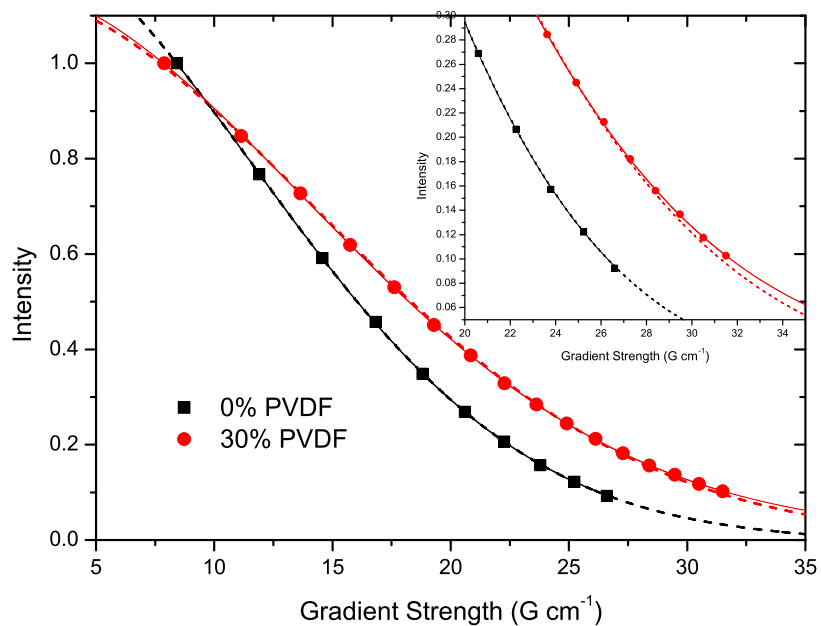


Figure 3: Intensity decay profile for  $^{19}\text{F}$  NMR self diffusion measurements for 0% (liquid electrolyte) and 30% PVDF/ PC/  $\text{LiBF}_4$  (1.0 M) polymer gel electrolytes at 303 K. The data in each case has been fitted with equation 1 (dashed line) and 5 (solid line), which represents a single and two diffusive species, respectively. Inset shows high gradient strengths to highlight deviance between the two fitting procedures.

phases, however it is difficult to accurately fit the data. It is reasonable to assume that if there are solvent molecules and lithium ions present in the solvated amorphous phase, then there are likely anions also present. In a previous publication it has been shown that in the liquid electrolytes the lithium ions are the largest entity, followed by the solvent molecules, with the smallest entity being the  $\text{BF}_4$  anion [40]. The detection of a second phase via diffusion measurements relies on there being a significant difference in value between the two phases, making them distinguishable. If the viscosity of the two phases were constant then as the size of the molecules decrease the diffusion of the two phases would converge, making them indistinguishable via NMR diffusion measurements. Therefore the  $^7\text{Li}$  measurements would display the biggest difference between the two phases and the  $^{19}\text{F}$  would be the most indistinguishable. Also as the polymer concentration is increased the proportion of the solvated amorphous PVDF would increase, which would also affect the ability to detect location of ions in two phases. This would explain the presence of a secondary phase located in all of the  $^1\text{H}$  30% PVDF gels but only some of the  $^1\text{H}$  20% PVDF gel measurements.

The diffusion constants obtained for the  $^{19}\text{F}$  NMR measurement on the 30% PVDF gel were 0.39 and 1.17 ( $10^{-10} \text{ m}^2 \text{ s}^{-1}$ ) with corresponding intensity values of 6% and 94%, respectively. Therefore the intensity from the solvated amorphous polymer phase is not very significant and it therefore proves difficult to accurately fit the data for the second phase. Therefore for the purpose of this publication it will be assumed that the  $\text{BF}_4$  anions are located in only the liquid electrolyte phase.

It has previously been shown that the size order of the constituents in the liquid electrolytes from NMR diffusion measurements is  $^{19}\text{F} < ^1\text{H} < ^7\text{Li}$ . This has been attributed to a large solvation shell around the lithium ions, which on average is around four PC molecules on per lithium cation [41], the fluorine ions were found to be unsolvated by the solvent molecules [42]. In order for two diffusive species to be distinguished via NMR diffusion measurements the viscosity of the two systems must be distinct, otherwise an average of the two phases will be observed.

Table 3 shows the  $^1\text{H}$  NMR diffusion constants for the liquid electrolyte and 20% and 30% PVDF/ PC/  $\text{LiBF}_4$  (0.3M and 1.0M) polymer gel electrolytes. As discussed above the  $^1\text{H}$  measurements were observed to exhibit two distinct phases for the 30% PVDF

Temp. (K)	Diffusion ( $\times 10^{-10} \text{ m}^2 \text{ s}^{-1}$ )							
	0.3M				1.0M			
	Liquid	20%	30%	30%	Liquid	20%	30%	30%
		Slow	Fast			Slow	Fast	
303	5.00	3.09	1.08	3.15	2.79	1.67	0.62	1.74
313	6.18	3.87	1.50	4.05	3.54	2.18	0.70	2.12
323	7.43	4.68	2.10	5.26	4.46	2.73	1.23	3.02
333	8.86	5.48	2.52	6.12	5.32	3.31	1.66	3.94
343	—	6.43	3.00	7.02	6.56	3.86	2.01	4.48

Table 3:  $^1\text{H}$  diffusion constants for liquid, 20% and 30% PVDF/ PC/  $\text{LiBF}_4$  polymer gel electrolytes with 0.3M and 1.0M  $\text{LiBF}_4$  salt concentrations.

gels but only a single phase in the 20% PVDF gels, therefore there is only one diffusion constant for the 20% PVDF gels.

Firstly observing the 20% PVDF single fit data, it can be readily observed that the liquid electrolyte diffusion constants are consistently larger than the corresponding gels at all temperatures. If the solvent molecules were contained only in a pure liquid electrolyte phase, then the liquid and gel diffusion constants should be comparable. The deviance here can be described by two likely factors, firstly, the value for the 20% PVDF gels are an average of solvent molecules found in both the liquid phase and the solvated amorphous PVDF phase therefore reducing the absolute value. Secondly, there is a decrease in free volume of the liquid when inside the polymer gel electrolytes, which would likely cause some restricted diffusion in smaller channels which would yield a lower diffusion constant. It is likely due to the first factor here, however all of the gel data was fitted with two diffusion constants, however, most of the 20%  $^1\text{H}$  data was fitted well with a single fit, and the introduction of the second exponential did not improve the fit to the data and therefore was not accurate to carry out. This effect is most likely due to there being a lower concentration of solvent molecules located in the secondary phase or similar values of the diffusion constants in both phases.

The 30% PVDF slow diffusive phase is attributed to the solvated amorphous polymer phase. Since this phase is likely to have a distinguishable viscosity difference when



compared to the liquid electrolyte phase, it would be expected to have a lower diffusion constant. It can be seen in table 3 that the solvated amorphous PVDF phase (30% slow) is consistently lower than the liquid phase (30% fast). The slower diffusion constant is usually no less than 25% of the corresponding faster phase, this strengthens the hypothesis that the slower of the two diffusion phases is indeed the solvated amorphous phase, as the molecules would still be relatively mobile.

A direct ratio of the solvated amorphous PVDF ( $D_{Slow}$ ) and liquid phase ( $D_{Fast}$ ) diffusion constants in table 3 for the 0.3M LiBF<sub>4</sub> sample are given as 0.343 and 0.427 at 303 K and 343 K, respectively. This result suggests that the diffusion of the <sup>1</sup>H containing molecules in the slower phase is increasing faster with temperature than the liquid electrolyte phase. The Stokes-Einstein equation is given by;

$$D = \frac{k_B T}{6\pi\eta r \xi} \quad (6)$$

where  $k_B$  is the Boltzmann constant,  $T$  is the absolute temperature of the system,  $\eta$  is the viscosity,  $r$  is the radius of the diffusing species and  $\xi$  is a factor which corrects for deviations away from a perfect spherical model. Therefore the ratio of  $D_{Slow}/D_{Fast}$  would take the form;

$$\frac{D_{Slow}}{D_{Fast}} = \frac{\eta_{Fast} r_{Fast} \xi_{Fast}}{\eta_{Slow} r_{Slow} \xi_{Slow}} \quad (7)$$

assuming that the parameter  $\xi$  is independent of temperature. If we also assume that the average radius of the diffusing species in each phase has a negligible change with temperature then the increase in the ratio must be due to a change in relative viscosity. This result therefore suggests that at higher temperatures the two mobile phases converge in terms of the viscosity. This conclusion would also rely on the structure of the gel to remain constant over the measured temperature range, however since the gel is far away from the melting temperature this is a reasonable assumption.

Table 4 displays the <sup>7</sup>Li NMR diffusion constants for both liquid electrolyte and 20% and 30% PVDF/ PC/ LiBF<sub>4</sub> (0.3M and 1.0M) polymer gel electrolytes. Similar to the <sup>1</sup>H results, the <sup>7</sup>Li NMR diffusion measurements exhibit two distinct environments within the polymer gel electrolytes. These have been also labeled "slow" and "fast" which correspond to the solvated amorphous PVDF phase and the liquid electrolyte phase, respectively. The diffusion of the liquid phase of the gels in the 20% and 30% PVDF gels

Temp(K)	Diffusion ( $\times 10^{-10} \text{ m}^2 \text{ s}^{-1}$ )									
	0.3M					1.0M				
	Liquid	20%	20%	30%	30%	Liquid	20%	20%	30%	30%
		Slow	Fast	Slow	Fast		Slow	Fast	Slow	Fast
283	1.22	—	—	0.25	1.00	0.61	0.24	0.55	0.11	0.46
293	1.64	—	—	0.35	1.33	0.86	0.29	0.63	0.23	0.91
303	2.17	0.69	1.94	0.48	1.82	1.19	0.41	0.88	0.27	0.94
313	2.75	0.97	2.45	0.56	2.06	1.56	0.53	1.13	0.29	1.02
323	3.35	1.18	3.13	0.72	2.42	1.97	0.59	1.35	0.35	1.25
333	4.06	1.52	3.65	0.89	2.96	2.44	0.81	1.64	0.55	1.74
343	5.63	1.75	4.14	1.06	3.23	2.96	0.93	1.92	0.65	2.03

Table 4:  $^7\text{Li}$  diffusion constants for liquid, 20% and 30% PVDF/ PC/  $\text{LiBF}_4$  polymer gel electrolytes with 0.3M and 1.0M  $\text{LiBF}_4$  salt concentrations.

are comparable suggesting that in each case the ions in the liquid phase are acting in the same manner regardless of polymer concentration. Taking for example the PVDF/ PC/  $\text{LiBF}_4$  (1.0M) sample at 313 K, the diffusion values are 1.56, 1.13 and 1.02 ( $10^{-10} \text{ m}^2 \text{ s}^{-1}$ ) for the liquid electrolyte, 20% PVDF gel liquid phase and 30% PVDF gel liquid phase, respectively. Therefore with the initial addition of the polymer there is a decrease in the diffusion which is attributed to the decrease in free volume for the ions and molecules to translate, however the decrease in diffusion of the liquid phase with a further increase in polymer is much less significant. This trend holds for all of the data displayed in table 4 and supports the theory that the faster diffusing phase corresponds to a pure liquid electrolyte phase.

Figure 4 shows the ratio of the solvated amorphous and liquid phase diffusion ( $D_{Slow}/D_{Fast}$ ) for the 20% and 30% PVDF/ PC/  $\text{LiBF}_4$  (1.0 M) polymer gel electrolytes. From figure 4 it can readily be observed that the ratio for both the  $^1\text{H}$  and  $^7\text{Li}$  measurements increases with increasing temperature. The sizes of the ions and solvent molecules are likely comparable in both phases. It is possible that the lithium cations are less solvated in the secondary solvated amorphous phase, which would change their radius and diffusion constant, however here it is assumed that the lithium-solvent molecules are stable and

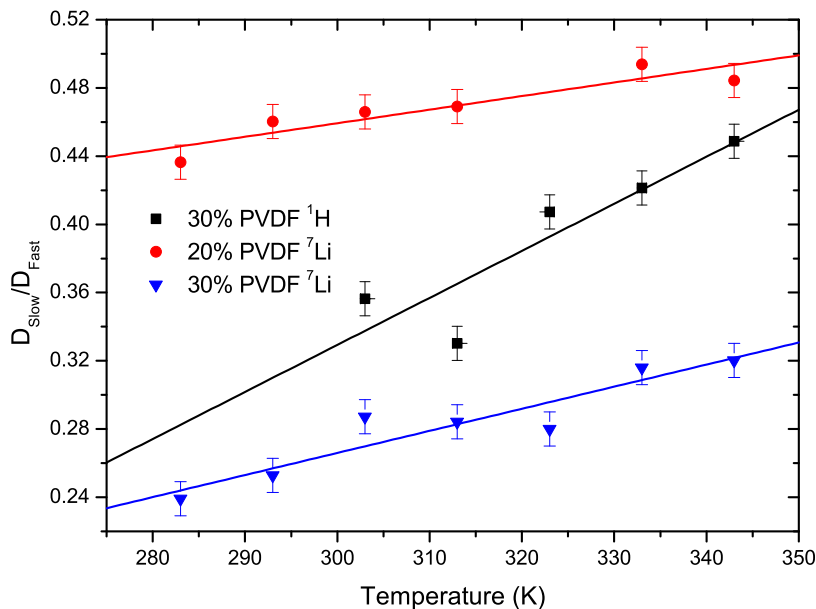


Figure 4: Ratio of diffusion constants for solvated amorphous PVDF phase ( $D_{Slow}$ ) and liquid phase ( $D_{Fast}$ )  $D_{Slow}/D_{Fast}$  for  $^1\text{H}$  and  $^7\text{Li}$  NMR self diffusion measurements for 20% and 30% PVDF/ PC/  $\text{LiBF}_4$  (1.0 M) polymer gel electrolytes. The data in each case has been fitted with a linear fit to highlight the positive gradient.

have comparable radii. This suggests that the viscosity of the solvated amorphous phase is converging with the pure liquid phase with increasing temperature.

Table 5 shows the  $^{19}\text{F}$  NMR diffusion measurements for the liquid electrolytes and 20% and 30% PVDF/ PC/  $\text{LiBF}_4$  (0.3M, 0.7M and 1.0M) polymer gel electrolytes. From previous work carried out on the liquid electrolytes it was found that the  $\text{BF}_4$  anions are not solvated by the solvent molecules, this results in their radius being relatively small [42]. This could be one explanation for the lack of presence in the solvated amorphous phase. Therefore, it is highly likely that there are some anions located in the solvated amorphous phase, which can not be accurately fitted due to the apparent similarity between the viscosities of the two phases. The results in table 5 are an average of all species within the polymer gel electrolyte. The liquid electrolyte diffusion constant measurements are again consistently higher than the corresponding gels, this is attributed to the anions in the solvated amorphous phase, which would be lower than the liquid phase reducing the overall value. The deviation between the liquid electrolyte data and

Temp. (K)	Diffusion ( $\times 10^{-10} \text{ m}^2 \text{ s}^{-1}$ )								
	0.3M			0.7M			1.0M		
	Liquid	20%	30%	Liquid	20%	30%	Liquid	20%	30%
283	2.18	1.92	1.80	1.26	1.14	0.98	0.86	0.65	0.59
293	2.87	2.54	2.22	1.71	1.47	1.31	1.19	0.86	0.86
303	3.64	3.11	3.02	2.25	1.79	1.65	1.60	1.11	1.08
313	4.52	3.68	3.55	2.84	2.14	2.04	2.07	1.37	1.41
323	5.59	4.42	4.17	3.56	2.51	2.34	2.55	1.66	1.67
333	7.02	5.01	4.61	4.71	2.89	2.67	3.25	2.01	1.87
343	8.12	5.64	4.98	5.46	3.23	2.96	3.94	2.36	2.12

Table 5:  $^{19}\text{F}$  diffusion constants for liquid, 20% and 30% PVDF/ PC/  $\text{LiBF}_4$  polymer gel electrolytes with 0.3M, 0.7M and 1.0M  $\text{LiBF}_4$  salt concentrations.

the liquid electrolyte gel phase increases at higher temperatures, which might suggest the presence of some restricted diffusion.

In previous studies the liquid electrolyte counterparts were analysed with Arrhenius plots in order to determine the temperature dependence of the diffusion measurements [40]. The same method will be applied here in order to compare the activation energies obtained for the polymer gel electrolytes. Figure 5 shows the  $^1\text{H}$ ,  $^7\text{Li}$  and  $^{19}\text{F}$  Arrhenius plot for the 20% PVDF/ PC/  $\text{LiBF}_4$  polymer gel electrolytes. The Arrhenius plot consists of taking the natural logarithm of diffusion and plotting it against  $1000/T$ . If the resulting trend is linear then the system is said to be displaying Arrhenius type temperature dependence, otherwise is considered non-Arrhenius and usually described by the Vogel-Fulcher-Tammann (VFT) equation [43, 44, 45]. The Arrhenius type behaviour is described by an equation of the form;

$$D = D_0 \exp \left[ -\frac{E_D}{RT} \right] \quad (8)$$

where  $E_D$  is the activation energy of diffusion,  $D_0$  is the diffusion at infinite temperature,  $R$  is the universal gas constant and  $T$  is the absolute temperature. The VFT equation is described in the form;

$$D = D_0 \exp \left[ -\frac{E'_D}{R(T - T_0)} \right] \quad (9)$$

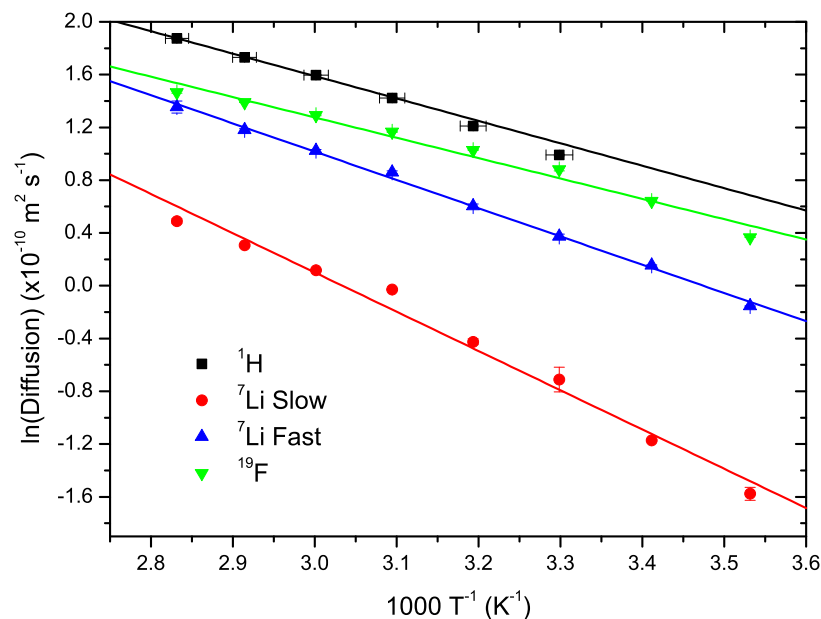


Figure 5: Arrhenius plot for  $^1\text{H}$ ,  $^7\text{Li}$  and  $^{19}\text{F}$  NMR self diffusion measurements for 20% PVDF/ PC/  $\text{LiBF}_4$  (0.5 M) polymer gel electrolytes. 'Slow' and 'Fast' phases refer to the solvated amorphous PVDF and liquid phases, respectively.

where  $T_0$  is the ideal glass transition temperature and  $E'_D$  is a temperature dependent energy term distinct from the activation energy in equation 8. VTF type dependence usually describes systems that are approaching their glass transition temperatures, it has been shown in previous studies that PC/  $\text{LiBF}_4$  liquid electrolytes exhibit Arrhenius type temperature dependence over the temperature range used in this study, however in the same paper it was shown that for the conductivity measurements below 273 K the trend was VTF [40]. Therefore for the data in this paper it is reasonable to assume that the liquid phase of the polymer gel electrolytes should exhibit Arrhenius type temperature dependence.

Figure 5 shows an Arrhenius plot for  $^1\text{H}$ ,  $^7\text{Li}$  and  $^{19}\text{F}$  NMR self diffusion measurements for 20% PVDF/ PC/  $\text{LiBF}_4$  (1.0 M) polymer gel electrolytes. It can be readily observed from figure 5 that all of the data can be fitted with linear lines, suggesting that all of the measurements have Arrhenius type temperature dependence in this temperature range. The activation energies obtained from figure 5 are  $(14.1 \pm 0.4)$  kJ mol<sup>-1</sup>,  $(24.7 \pm 0.9)$  kJ

mol<sup>-1</sup>, (17.8±0.4) kJ mol<sup>-1</sup> and (12.8±0.8) kJ mol<sup>-1</sup> for the <sup>1</sup>H, <sup>7</sup>Li slow, <sup>7</sup>Li fast and <sup>19</sup>F, respectively. A high activation energy means that the entity is requiring more energy to translate and therefore is either in a more viscous medium or has a larger radius. From the four values taken from figure 5 it can be readily noted that the fluorinated BF<sub>4</sub> anions have the lowest activation energy. It is fair to assume that the <sup>1</sup>H, <sup>7</sup>Li fast and <sup>19</sup>F values are all within the same medium and therefore share a common bulk viscosity since they are all located in the liquid phase. Therefore from the activation energies a size order can be determined, to be <sup>19</sup>F < <sup>1</sup>H < <sup>7</sup>Li. This size order was observed in the PC/ LiBF<sub>4</sub> liquid electrolytes and was attributed to the the lithium ions having a large solvation shell of around 3-4 solvent molecules on average [41, 40]. Since the diffusion measured is an average of all species in the liquid phase the hydrogen measurement has a smaller radius than the lithium ions because although it is part of the solvation shell, there are also lots of free solvent molecules, effectively reducing the average radius. It has been seen in previous work that the fluorinated BF<sub>4</sub> anion does not get solvated by the PC molecules and therefore usually has a radius of around 0.229 nm [46]. However the BF<sub>4</sub> anions can associate with the lithium ions in favour if the solvent molecules which will increase their radius by a small amount.

It is possible to compare the two different lithium ion phases in the polymer gel electrolyte by considering the relevant activation energies. The values as quoted above from figure 5 are (14.1±0.4) kJ mol<sup>-1</sup> and (24.7±0.9) kJ mol<sup>-1</sup> for the liquid electrolyte phase and the solvated amorphous phases, respectively. The activation energy of the solvated amorphous phase is significantly higher than the liquid electrolyte phase. Since in each of these phases it is likely that the same species are contained (i.e. LiBF<sub>4</sub> ion pairs and various solvated lithium ions), the average radius would be comparable. Therefore this significant difference in activation energies is likely due to a difference in viscosity between the two phases. The same conclusion was reached from observing the ratio of the diffusion from the solvated amorphous and liquid electrolyte phases (figure 4).

Figure 6 shows the Arrhenius plot for the 30% PVDF/ PC/ LiBF<sub>4</sub> (0.5M) polymer gel electrolytes for the <sup>1</sup>H, <sup>7</sup>Li and <sup>19</sup>F nuclei. As with the 20% PVDF gels all of the plots show a linear relationship over the temperature range measured (293-343 K), which allows for the determination of an activation energy. The energies obtained from figure

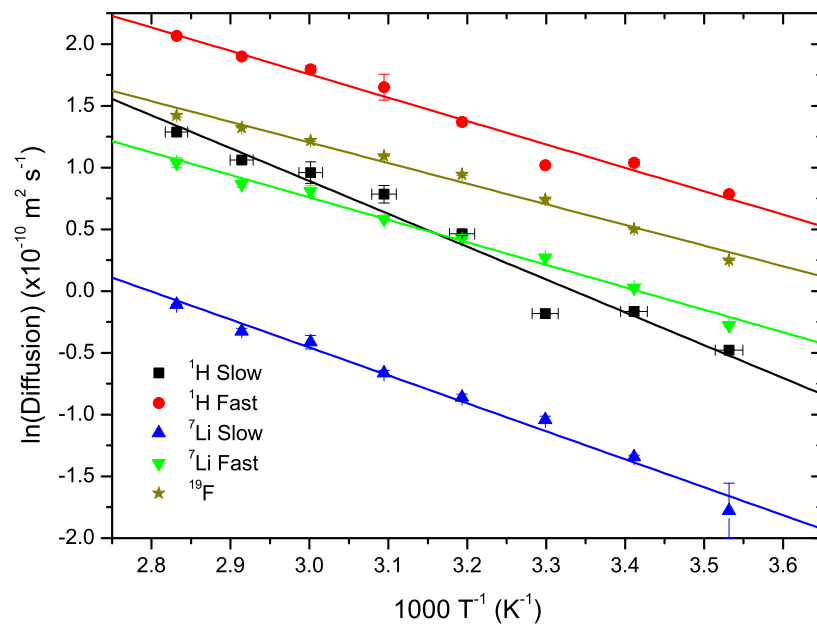


Figure 6: Arrhenius plot for  $^1\text{H}$ ,  $^7\text{Li}$  and  $^{19}\text{F}$  NMR self diffusion measurements for 30% PVDF/ PC/  $\text{LiBF}_4$  (0.5 M) polymer gel electrolytes. 'Slow' and 'Fast' phases refer to the solvated amorphous PVDF and liquid phases, respectively.

6 are  $(22\pm 1)$  kJ mol<sup>-1</sup>,  $(16\pm 1)$  kJ mol<sup>-1</sup>,  $(18.8\pm 0.9)$  kJ mol<sup>-1</sup>,  $(15.1\pm 0.6)$  kJ mol<sup>-1</sup> and  $(13.9\pm 0.7)$  kJ mol<sup>-1</sup> for the <sup>1</sup>H slow, <sup>1</sup>H fast, <sup>7</sup>Li slow, <sup>7</sup>Li fast and <sup>19</sup>F, respectively. Firstly looking at the liquid electrolyte phases it can be observed again that the size order is <sup>19</sup>F < <sup>1</sup>H ≈ <sup>7</sup>Li, this time the hydrogen activation energy is slightly higher than the lithium one suggesting that it may be larger. It should also be noted that the two values for the solvated amorphous phases are again significantly larger than the corresponding liquid counterpart, suggesting that there is a noticeable viscosity difference between the two phases. It is clear that there are ions present in both the solvated amorphous PVDF and liquid electrolyte phases, however, it is important to understand whether the conductivity arises from both phases or just the liquid electrolyte phase. This will be addressed in a subsequent paper, which addresses the conductivity of the polymer gel electrolytes and comparing them to the diffusion measurements presented here[28]. In this subsequent paper it is concluded that there is evidence to suggest that the ionic conductivity arises from not only the pure liquid phase but also the solvated amorphous phase [28].

When fitting the diffusion decay curves with equation 5 the intensity values were determined which gives an indication of the relevant contribution from each phase. For both the <sup>7</sup>Li and <sup>1</sup>H measurements the intensity values were observed to not have a trend with either temperature or salt concentration. Therefore it was possible to take an average over all these measurements to obtain a universal value for each polymer concentration. The average value for the <sup>7</sup>Li 20% PVDF/ PC/ LiBF<sub>4</sub> measurements is  $(0.66\pm 0.01)$ , which corresponds to the liquid electrolyte (fast) phase representing 66% of the signal with the remaining 34% being from the solvated amorphous PVDF phase; the intensity values have been normalised to add to one so that they represent a percentage. The intensity value for the <sup>7</sup>Li 30% PVDF/ PC/ LiBF<sub>4</sub> polymer gel measurements is  $(0.61\pm 0.01)$ , corresponding to 61% liquid contribution and 39% solvated amorphous PVDF phase. The increase in polymer concentration has caused the intensity values to shift resulting in a stronger contribution from the solvated amorphous PVDF phase. This result is reasonable as the increase in polymer would likely cause more solvated amorphous phase locations within the polymer gel electrolytes.

The intensity values were also determined for the <sup>1</sup>H measurements of the 30% PVDF/



	$T_2$ (ms)			Intensity (%)		
	$T_1^1$	$T_1^2$	$T_1^3$	$I_1$	$I_2$	$I_3$
1 fit	297	—	—	100	—	—
2 fit	399	76	—	59	41	—
3 fit	419	107	22	52	36	12.7

Table 6:  $^1\text{H}$  transverse relaxation time ( $T_2$ ) fitting parameters for 20% PVDF/ PC/  $\text{LiBF}_4$  (0.5M) polymer gel electrolytes shown in figure 7.

PC/  $\text{LiBF}_4$  polymer gel electrolytes. The intensity for the liquid electrolyte phase is  $(0.59 \pm 0.01)$ , which corresponds to 59% of the signal arising from the liquid electrolyte phase and the remaining 41% from the solvated amorphous PVDF phase. This value is comparable to the lithium value for the 30% PVDF polymer gel electrolyte, suggesting there is an even distribution of the lithium and hydrogen containing species in the two phases. However, this is clearly not the case for the fluorine NMR measurements, as fitting a second exponential term to the  $^{19}\text{F}$  data was difficult.

#### 4. NMR Relaxation Times

Transverse relaxation measurements have been taken for the  $^1\text{H}$  and  $^7\text{Li}$  nuclei for the 20% and 30% PVDF/ PC/  $\text{LiBF}_4$  polymer gel electrolytes. Multiple environments have been observed from transverse relaxation measurements for the  $^7\text{Li}$  nuclei [17] and from  $T_{1\rho}$  measurements for the  $^1\text{H}$  nuclei from our previous research at the University of Leeds[27]. It was concluded that for the  $^1\text{H}$  measurements that there are at least four phases; a crystalline PVDF lamellae phase, inter-lamellae amorphous PVDF phase, solvated amorphous PVDF phase and a liquid electrolyte phase [27]. Figure 7 shows an example  $^1\text{H}$   $T_2$  decay curve for the 20% PVDF/ PC/  $\text{LiBF}_4$  polymer gel electrolyte. The data has been fitted initially with equation 3 (green line); it can readily be observed that the fit is insufficient to describe the data.

Since the data in figure 7 could not be fitted with equation 3 subsequent exponential terms have been added in series to describe the other phases present in the form of;

$$M_{xy}(t) = M_0^1 \exp\left[\frac{-t}{T_1^1}\right] + M_0^2 \exp\left[\frac{-t}{T_2^2}\right] \quad (10)$$

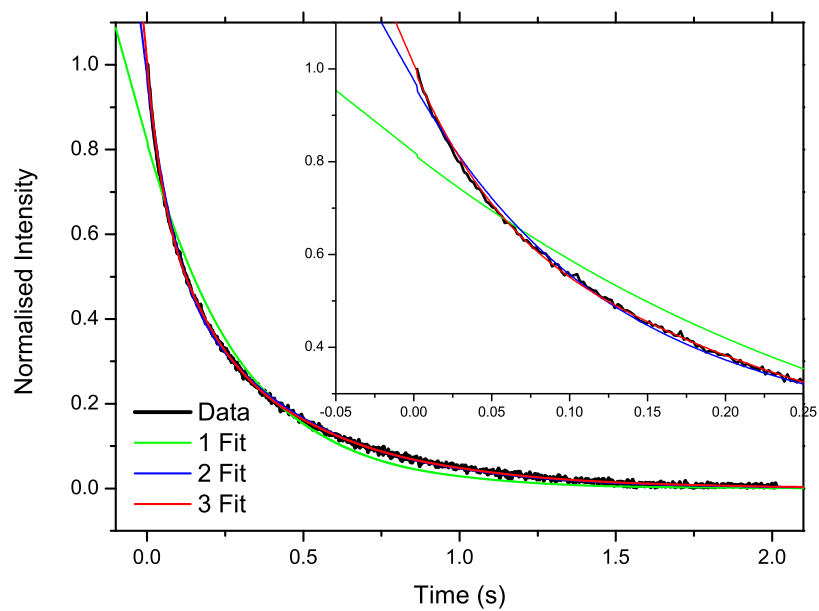


Figure 7:  $T_2$  decay curve for  $^1\text{H}$  NMR relaxation time measurements for 20% PVDF/ PC/  $\text{LiBF}_4$  (0.5M) polymer gel electrolytes at 303 K. The '1 Fit', '2 Fit' and '3 Fit' lines have been fitted with equations 3, 10 and 11, respectively. The inset shows the data at low times in order to differentiate between the three fitting procedures.

and

$$M_{xy}(t) = M_0^1 \exp\left[\frac{-t}{T_2^1}\right] + M_0^2 \exp\left[\frac{-t}{T_2^2}\right] + M_0^3 \exp\left[\frac{-t}{T_2^3}\right] \quad (11)$$

where  $T_2^1$ ,  $T_2^2$  and  $T_2^3$  are the transverse relaxation times of each phase,  $M_0^1$ ,  $M_0^2$  and  $M_0^3$  represent the relative contribution from each phase.

The data in figure 7 has been fitted with equations 10 (blue line) and 11 (red line), it can be seen that with the addition of a second exponential term the fit to the data is greatly enhanced, however, at very low times the fit deviates from the data. The addition of the third exponential term accounts for this and likely represents another phase within the polymer gel electrolytes. The inset of figure 7 shows the data at short times in order to highlight the difference between the three fitted lines. The fitting parameters from figure 7 are summarised in table 6. The  $T_2$  values obtained from figure 7 are  $(297 \pm 2)$  ms for single exponential fit,  $(399 \pm 2)$  ms and  $(76 \pm 1)$  ms for the double exponential fit and  $(419 \pm 2)$  ms,  $(107 \pm 3)$  ms and  $(22 \pm 2)$  ms for the three exponential term fit. It was not possible to fit anymore exponential terms to the data and therefore the gels in this instance are considered to have three distinct phases. It is likely that there are four phases present as listed above, however the crystalline PVDF  $T_2$  value is known to be around 20  $\mu$ s [47], which is significantly lower than the lowest  $T_2$  measured here. Therefore the three phases detected are assumed to be the inter-lamellae amorphous PVDF phase, solvated amorphous phase and liquid electrolyte phases. The intensity of the fits from figure 7 were determined to be 12.7%, 35.7% and 51.6%, which corresponds to contributions from the inter-lamellae amorphous PVDF phase, solvated amorphous phase and liquid electrolytes phase, respectively. As indicated by the diffusion measurements, the most significant phase is the pure liquid electrolyte phase.

Figure 8 shows a  $^1\text{H}$   $T_2$  decay curve for a 30% PVDF/ PC/  $\text{LiBF}_4$  polymer gel electrolyte, the fitting parameters for the three different fits have been summarised in table 7. The data has again been fitted with equations 3, 10 and 11 to identify the number of phases present. The  $T_2$  values obtained from figure 8 are  $(173 \pm 2)$  ms for single exponential fit and  $(255 \pm 1)$  ms and  $(41 \pm 1)$  ms for the double exponential fit. The  $T_2$  values obtained from equation 11 were determined as  $(263 \pm 2)$  ms,  $(49 \pm 1)$  ms and  $(5.1 \pm 0.5)$  ms representing the liquid electrolyte phase, solvated amorphous PVDF phase and inter-lamellae amorphous PVDF phase, respectively. As with the 20% PVDF gels

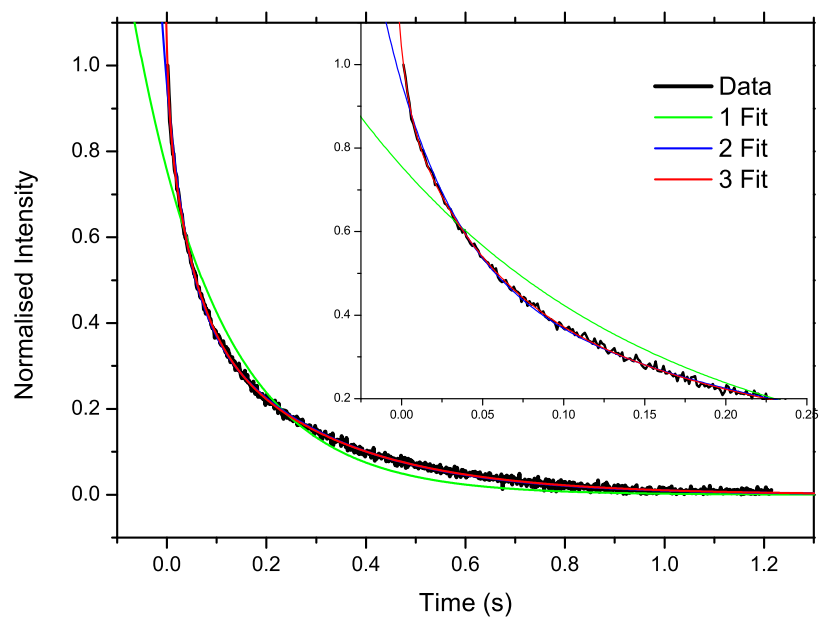


Figure 8:  $T_2$  decay curve for  $^1\text{H}$  NMR relaxation time measurements for 30% PVDF/ PC/  $\text{LiBF}_4$  (0.5M) polymer gel electrolytes at 303 K. The '1 Fit', '2 Fit' and '3 Fit' lines have been fitted with equations 3, 10 and 11, respectively. The inset shows the data at low times in order to differentiate between the three fitting procedures.

	$T_2$ (ms)			Intensity (%)		
	$T_1^1$	$T_1^2$	$T_1^3$	$I_1$	$I_2$	$I_3$
1 fit	173	—	—	100	—	—
2 fit	255	41	—	51	49	—
3 fit	263	49	5.1	44	42	14

Table 7:  $^1\text{H}$  transverse relaxation time ( $T_2$ ) fitting parameters for 30% PVDF/ PC/  $\text{LiBF}_4$  (0.5M) polymer gel electrolytes shown in figure 8.

only three phases were detected, this was again attributed to very small timescale of the crystalline PVDF. The intensities for these fits were determined as 44%, 42% and 14% for the liquid electrolyte, solvated amorphous PVDF and inter-lamellae amorphous PVDF phases, respectively. Therefore with the addition of more polymer to the system the intensities of the two polymer containing phases has increased and the liquid region has decreased in volume.

The average intensities for the  $^1\text{H}$  diffusion measurements for the 30% PVDF gels were reported above to be 59% and 41% for the liquid and solvated amorphous PVDF phases, respectively. The inter-lamellae amorphous PVDF phase was not present in the diffusion measurements because the diffusion constants are significantly smaller than for the mobile phases so were difficult to detect at these timescales. Therefore if the inter-lamellae amorphous PVDF phase  $T_2$  measurements are ignored the contributions for the two remaining phases become 51%. and 49% for the liquid and solvated amorphous PVDF phase, respectively; therefore the values obtained from the diffusion and  $T_2$  measurements are comparable.

Figure 9 displays a  $^7\text{Li}$   $T_2$  decay curve for 20% PVDF/ PC/  $\text{LiBF}_4$  (1.0M) at 303 K. Unlike the  $^1\text{H}$  measurements displayed in figures 7 and 8 the lithium data only required two exponential terms to accurately fit the data. The inset of figure 9 has been included to highlight the deviation of the two fits. It can be readily noted that the single exponential term is insufficient, which indicates that there are two distinct phases containing lithium ions. This correlates with the diffusion measurements, which also exhibited two distinct phases. The fitting parameters for the two parameter fit have been summarised in table 8. The  $T_2$  values obtained from figure 9 are  $(807\pm 15)$  ms and  $(379\pm 10)$  ms for the liquid

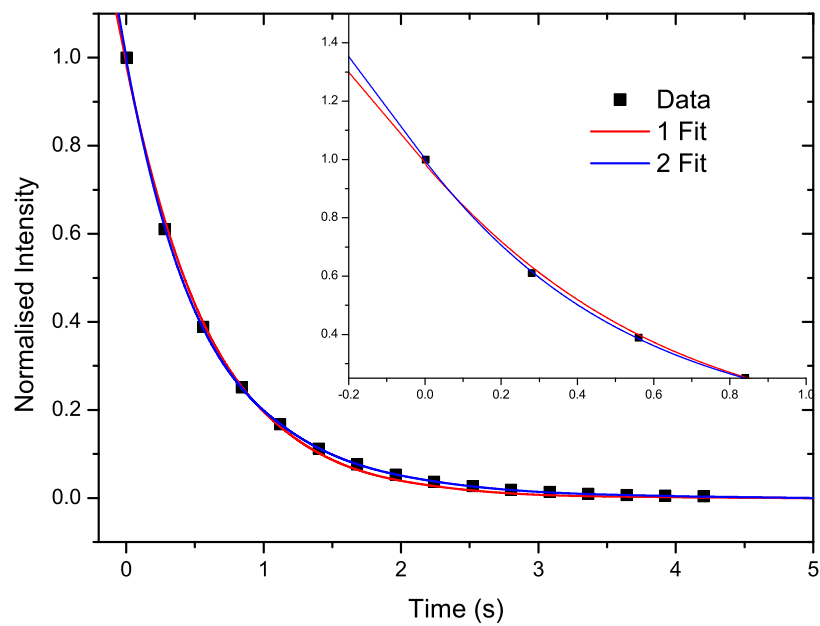


Figure 9:  $T_2$  decay curve for  $^7\text{Li}$  NMR relaxation time measurements for 20% PVDF/ PC/  $\text{LiBF}_4$  (1.0M) polymer gel electrolytes at 303 K. The '1 Fit' and '2 Fit' lines have been fitted with equations 3 and 10, respectively. The inset shows the data at low times in order to differentiate between the two fitting procedures.

PVDF Conc. (%wt.)	$T_2$ (ms)		Intensity (%)	
	$T_1^1$	$T_1^2$	$I_1$	$I_2$
20	807	379	58	42
30	837	255	64	36

Table 8:  $^7\text{Li}$  transverse relaxation time ( $T_2$ ) fitting parameters for 20% (from figure 9) and 30% (from figure 10) PVDF/ PC/  $\text{LiBF}_4$  (0.5M) polymer gel electrolytes.

electrolyte and solvated amorphous PVDF phases, respectively. The liquid electrolyte phase contributed 58% to the total decay, determined from the fitting of equation 10. The contribution from the liquid electrolyte phase for the diffusion measurements was given as 66% and is therefore comparable to the  $T_2$  result.

Figure 10 displays a  $^7\text{Li}$   $T_2$  decay curve for 30% PVDF/ PC/  $\text{LiBF}_4$  (1.0M) at 303 K. As with the 20% PVDF gel measurements, the 30% gels are well described with the introduction of the second exponential term. The values of  $T_2$  obtained from figure 10 are  $(837\pm 16)$  ms and  $(255\pm 12)$  ms with relative intensities 64% and 36% for the liquid electrolyte and solvated amorphous PVDF phases, respectively. Therefore the liquid accounts for 64% of the total decay, this is comparable to the 61% contribution from the liquid phase determined from the diffusion measurements.

The lithium measurements give a strong indication that there are lithium ions present in two distinct phases, which have been attributed to the liquid electrolyte and solvated amorphous PVDF phases. However, an issue not addressed in this publication is the conductivity contribution, and whether the lithium ions in the solvated amorphous polymer phase contribute to the total conductivity or not. This will be addressed in a subsequent paper which will focus on the conductivity results and comparing them to the diffusion results presented in this publication[28], in which we conclude that there is a strong indication that the lithium ions in both phases contribute to the overall conductivity.

## 5. Conclusions

In this publication NMR self diffusion measurements have been conducted for 20% and 30% PVDF/ PC/  $\text{LiBF}_4$  polymer gel electrolytes using the  $^1\text{H}$ ,  $^7\text{Li}$  and  $^{19}\text{F}$  nuclei.

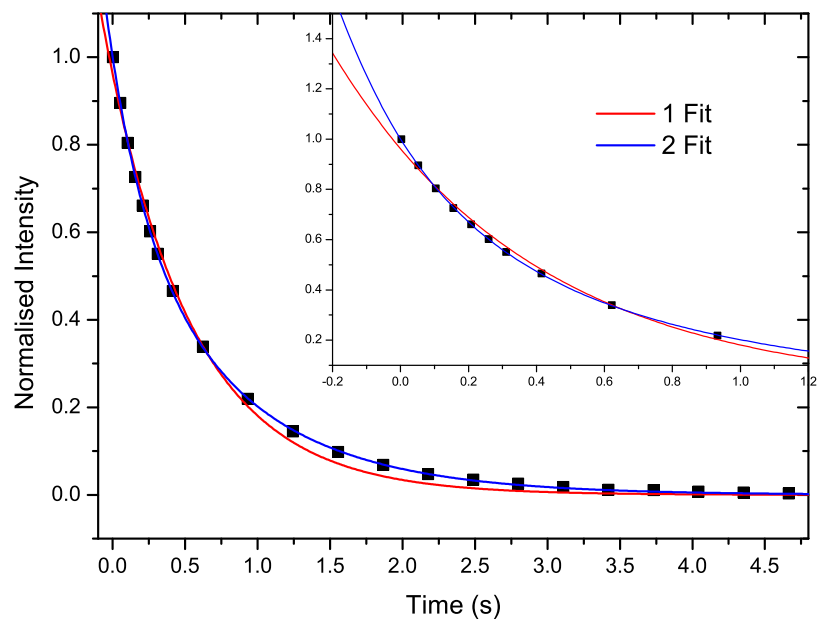


Figure 10:  $T_2$  decay curve for  $^7\text{Li}$  NMR relaxation time measurements for 30% PVDF/ PC/  $\text{LiBF}_4$  (1.0M) polymer gel electrolytes at 303 K. The '1 Fit' and '2 Fit' lines have been fitted with equations 3 and 10, respectively. The inset shows the data at low times in order to differentiate between the two fitting procedures.



The  $^1\text{H}$  nucleus will detect the hydrogen on the solvent molecules and also the polymer backbone, the  $^7\text{Li}$  nucleus will detect the lithium ions and the  $^{19}\text{F}$  nucleus will detect the  $\text{BF}_4$  anion and fluorine on the PVDF backbone.

The diffusion measurements for the  $^1\text{H}$  and  $^7\text{Li}$  exhibit two distinct diffusive regions within the polymer gel electrolyte, which have been attributed to the liquid electrolyte phase and solvated amorphous phase of the gel. The  $^{19}\text{F}$  diffusion measurements showed some indication of a second phase, however not strong enough to fit confidently. Therefore for the duration of this publication it was assumed that the  $\text{BF}_4$  anions were located solely in the liquid electrolyte phase.

The diffusion measurements were taken with varying temperature and salt concentration. The diffusion constants were observed in general to decrease with increasing salt concentration and increase with temperature, which was attributed to viscosity effects. The order of the diffusion constants were  $^{19}\text{F} < ^1\text{H} \approx ^7\text{Li}$ , suggesting that this was also the size order as all diffusing species have the same viscosity. This order was also observed for liquid electrolyte measurements taken previously [40].

All diffusion measurements were observed to exhibit Arrhenius type temperature behaviour. Therefore activation energies were determined for the three nuclei, for the  $^1\text{H}$  and  $^7\text{Li}$  measurements, both the liquid and solvated amorphous PVDF phase were determined. The activation energies for the solvated amorphous phase were significantly higher than for the corresponding liquid electrolyte phase, suggesting that the viscosity of the solvated amorphous phase is significantly higher than the liquid phase. A ratio of the solvated amorphous PVDF ( $D_{Slow}$ ) and liquid phase ( $D_{Fast}$ ) diffusion constants ( $D_{Slow}/D_{Fast}$ ) was found to increase with increasing temperature, indicating that the viscosity of the two phases is converging at elevated temperatures.

Transverse relaxation ( $T_2$ ) measurements have been taken using the  $^1\text{H}$  and  $^7\text{Li}$  nuclei for both 20% and 30% PVDF/ PC/  $\text{LiBF}_4$  polymer gel electrolytes. The fitting of the  $^1\text{H}$   $T_2$  decay curve shows three distinct phases within the gels. These have been attributed to the inter-lamellae amorphous PVDF, solvated amorphous PVDF phase and liquid electrolyte phase. The crystalline PVDF phase, observed in  $T_{1\rho}$  measurements previously carried out at the University of Leeds [27] was not observed as it occurs on timescales around 20  $\mu\text{s}$  [47], which is significantly lower than the machines capability. The  $^7\text{Li}$

$T_2$  decay curves show two distinct phases in the gels containing lithium ions which have been attributed to the solvated amorphous PVDF and the liquid electrolyte phases.

The intensities from both the diffusion and  $T_2$  measurements are comparable, strongly suggesting that there are lithium ions located in two phases in the polymer gel electrolytes. In a subsequent publication we will assess the likelihood that the ions within the solvated amorphous phase contribute to the bulk conductivity of the sample by comparing the diffusion constants measured in this publication with ionic conductivity measurements of the polymer gel electrolytes[28].

### 5.1. Acknowledgments

The authors would like to thank Dr R. Damion for help with the setting up of the NMR probes and coils for the NMR diffusion measurements, Mr S. Wellings for help with glove box operations and EPSRC for funding the studentship for PM Richardson.

## References

- [1] MB Armand, JM Chabagno, MJ Duclot, P Vashishta, JN Mundy, and GK Shenoy. Fast ion transport in solids. *Eds. Vashishta, P., Mundy, JN & Shenoy, G. K, North Holland, Amsterdam, 1979.*
- [2] M Armand. Polymer solid electrolytes-an overview. *Solid State Ionics*, 9:745–754, 1983.
- [3] DE Fenton, JM Parker, and PV Wright. Complexes of alkali metal ions with poly (ethylene oxide). *Polymer*, 14(11):589, 1973.
- [4] PV Wright. Recent trends in polymer electrolytes based on poly (ethylene oxide). *Journal of Macromolecular Science Chemistry*, 26(2-3):519–550, 1989.
- [5] JY Song, YY Wang, and CC Wan. Review of gel-type polymer electrolytes for lithium-ion batteries. *Journal of Power Sources*, 77(2):183–197, 1999.
- [6] AM Stephan and KS Nahm. Review on composite polymer electrolytes for lithium batteries. *Polymer*, 47(16):5952–5964, 2006.
- [7] E Quartarone and P Mustarelli. Electrolytes for solid-state lithium rechargeable batteries: recent advances and perspectives. *Chemical Society Reviews*, 40(5):2525–2540, 2011.
- [8] Ian M Ward and Hugh V St A Hubbard. Polymer gel electrolytes: Conduction mechanism and battery applications. *Ionic Interactions in Natural and Synthetic Macromolecules*, pages 817–840, 2012.
- [9] IM Ward, HV St A Hubbard, SC Wellings, GP Thompson, J Kaschmitter, and HP Wang. Separator-free rechargeable lithium ion cells produced by the extrusion lamination of polymer gel electrolytes. *Journal of power sources*, 162(2):818–822, 2006.

- [10] PG Hall, GR Davies, JE McIntyre, IM Ward, DJ Bannister, and KMF Le Brocq. Ion conductivity in polysiloxane comb polymers with ethylene glycol teeth. *Polymer communications*, 27(4):98–100, 1986.
- [11] DJ Bannister, GR Davies, IM Ward, and JE McIntyre. Ionic conductivities of poly (methoxy polyethylene glycol monomethacrylate) complexes with liso 3 ch 3. *Polymer*, 25(11):1600–1602, 1984.
- [12] SA Dobrowski, GR Davies, JE McIntyre, and IM Ward. Ionic conduction in poly (n, n-dimethylacrylamide) gels complexing lithium salts. *Polymer*, 32(16):2887–2891, 1991.
- [13] AM Voice, JP Southall, V Rogers, KH Matthews, GR Davies, JE McIntyre, and IM Ward. Thermoreversible polymer gel electrolytes. *Polymer*, 35(16):3363–3372, 1994.
- [14] JP Southall, HV St A Hubbard, SF Johnston, V Rogers, GR Davies, JE McIntyre, and IM Ward. Ionic conductivity and viscosity correlations in liquid electrolytes for incorporation into pvdf gel electrolytes. *Solid State Ionics*, 85(1):51–60, 1996.
- [15] MJ Williamson, JP Southall, HV St A Hubbard, GR Davies, and IM Ward. Pulsed field gradient nmr diffusion measurements on electrolyte solutions containing licf 3 so 3. *Polymer*, 40(14):3945–3955, 1999.
- [16] H Kataoka, Y Saito, Y Miyazaki, and S Deki. Ionic mobilities of pvdf-based polymer gel electrolytes as studied by direct current nmr. *Solid state ionics*, 152:175–179, 2002.
- [17] A Magistris, E Quartarone, P Mustarelli, Y Saito, and H Kataoka. Pvdf-based porous polymer electrolytes for lithium batteries. *Solid State Ionics*, 152:347–354, 2002.
- [18] PM Richardson, AM Voice, and IM Ward. Two distinct lithium diffusive species for polymer gel electrolytes containing libf4, propylene carbonate (pc) and pvdf. *International Journal of Hydrogen Energy*, 39(6):2904–2908, 2014.
- [19] Claudio Capiglia, Yuria Saito, Hiroshi Kataoka, Teruo Kodama, Eliana Quartarone, and Piercarlo Mustarelli. Structure and transport properties of polymer gel electrolytes based on pvdf-hfp and lin (c 2 f 5 so 2) 2. *Solid State Ionics*, 131(3):291–299, 2000.
- [20] Yuria Saito, Hiroshi Kataoka, Claudio Capiglia, and Hitoshi Yamamoto. Ionic conduction properties of pvdf-hfp type gel polymer electrolytes with lithium imide salts. *The Journal of Physical Chemistry B*, 104(9):2189–2192, 2000.
- [21] H Ye, J Huang, JJ Xu, A Khalfan, and SG Greenbaum. Li ion conducting polymer gel electrolytes based on ionic liquid/pvdf-hfp blends. *Journal of the Electrochemical Society*, 154(11):A1048–A1057, 2007.
- [22] GP Pandey, RC Agrawal, and SA Hashmi. Magnesium ion-conducting gel polymer electrolytes dispersed with nanosized magnesium oxide. *Journal of Power Sources*, 190(2):563–572, 2009.
- [23] BS Kim, ST Baek, KW Song, IH Park, JO Lee, and N Nemoto. Thermoreversible gelation of poly (vinylidene fluoride) in propylene carbonate. *Journal of Macromolecular Science, Part B*, 43(4):741–754, 2004.
- [24] H Shimizu, Y Arioka, M Ogawa, R Wada, and M Okabe. Sol-gel transitions of poly (vinylidene fluoride) in organic solvents containing libf4. *Polymer journal*, 43(6):540–544, 2011.

- [25] CM Chou and PD Hong. Scattering modeling of nucleation gels. *Macromolecules*, 41(17):6540–6545, 2008.
- [26] CM Chou and PD Hong. A novel aspect on structural formation of physical gels. *Macromolecules*, 36(19):7331–7337, 2003.
- [27] HV St A Hubbard and IM Ward. Polymer gel composition studies using  $t1\rho$  nmr. *Polymer Preprints*, 49(1):709, 2008.
- [28] PM Richardson, AM Voice, and IM Ward. Ionic transport properties of poly(vinylidene fluoride) (PVDF) based polymer gel electrolytes containing LiBF<sub>4</sub> and propylene carbonate. *Electrochimica Acta*, submitted, 2015.
- [29] MJ Williamson, HV St A Hubbard, and IM Ward. Nmr measurements of self diffusion in polymer gel electrolytes. *Polymer*, 40(26):7177–7185, 1999.
- [30] IM Ward, MJ Williamson, HV St A Hubbard, JP Southall, and GR Davies. Nmr studies of ionic mobility in polymer gel electrolytes for advanced lithium batteries. *Journal of power sources*, 81:700–704, 1999.
- [31] K Hayamizu, Y Aihara, S Arai, and WS Price. Self-diffusion coefficients of lithium, anion, polymer, and solvent in polymer gel electrolytes measured using <sup>7</sup>Li, <sup>19</sup>F, and <sup>1</sup>H pulsed-gradient spin-echo NMR. *Electrochimica acta*, 45(8):1313–1319, 2000.
- [32] Y Saito, H Kataoka, and AM Stephan. Investigation of the conduction mechanisms of lithium gel polymer electrolytes based on electrical conductivity and diffusion coefficient using nmr. *Macromolecules*, 34(20):6955–6958, 2001.
- [33] Tatsuya Umecky, Yuria Saito, and Hajime Matsumoto. Direct measurements of ionic mobility of ionic liquids using the electric field applying pulsed gradient spin-echo nmr. *The Journal of Physical Chemistry B*, 113(25):8466–8468, 2009.
- [34] Yuria Saito, Miki Okano, Keigo Kubota, Tetsuo Sakai, Junji Fujioka, and Tomohiro Kawakami. Evaluation of interactive effects on the ionic conduction properties of polymer gel electrolytes. *The Journal of Physical Chemistry B*, 116(33):10089–10097, 2012.
- [35] RM Cotts, MJR Hoch, T Sun, and JT Markert. Pulsed field gradient stimulated echo methods for improved nmr diffusion measurements in heterogeneous systems. *Journal of Magnetic Resonance (1969)*, 83(2):252–266, 1989.
- [36] EO Stejskal and JE Tanner. Spin diffusion measurements: spin echoes in the presence of a time-dependent field gradient. *The journal of chemical physics*, 42(1):288–292, 1965.
- [37] MJ Williamson, JP Southall, HV St A Hubbard, Sean F Johnston, GR Davies, and IM Ward. Nmr measurements of ionic mobility in model polymer electrolyte solutions. *Electrochimica acta*, 43(10):1415–1420, 1998.
- [38] S Meiboom and D Gill. Modified spin-echo method for measuring nuclear relaxation times. *Review of scientific instruments*, 29(8):688–691, 1958.
- [39] EL Hahn. Spin echoes. *Physical Review*, 80(4):580, 1950.
- [40] PM Richardson, AM Voice, and IM Ward. Pulsed-field gradient nmr self diffusion and ionic conductivity measurements for liquid electrolytes containing libf<sub>4</sub> and propylene carbonate. *Electrochimica*

- Acta*, 130:606–618, 2014.
- [41] Haruhiko Ohtani, Yasukazu Hirao, Akihiro Ito, Kazuyoshi Tanaka, and Osamu Hatozaki. Theoretical study on thermochemistry of solvated lithium-cation with propylene carbonate. *Journal of thermal analysis and calorimetry*, 99(1):139–144, 2010.
  - [42] Howard L Yeager, John D Fedyk, and Richard J Parker. Spectroscopic studies of ionic solvation in propylene carbonate. *The Journal of Physical Chemistry*, 77(20):2407–2410, 1973.
  - [43] H Vogel. The temperature dependence law of the viscosity of fluids. *Phys. Z*, 22:645–646, 1921.
  - [44] GS Fulcher. Analysis of recent measurements of the viscosity of glasses. *Journal of the American Ceramic Society*, 8(6):339–355, 1925.
  - [45] G Tammann and W Hesse. The dependency of viscosity on temperature in hypothermic liquids. *Zeitschrift Fur Anorganische Und Allgemeine Chemie*, 156(4), 1926.
  - [46] Makoto Ue. Mobility and ionic association of lithium and quaternary ammonium salts in propylene carbonate and  $\gamma$ -butyrolactone. *Journal of the electrochemical society*, 141(12):3336–3342, 1994.
  - [47] DC Douglass, VJ McBrierty, and TT Wang. The use of nmr linewidths to study b-axis distributions in poled and unpoled pvdf. *The Journal of Chemical Physics*, 77(11):5826–5835, 1982.

## Highlights

- Temperature and salt concentration study of PVDF/ PC/ LiBF<sub>4</sub> polymer gel electrolytes.
- Lithium ions were found to be located in two distinct phases in the gel structure.
- Pulse field gradient diffusion and transverse relaxation measurements both confirm lithium ion location in two mobile liquid-like phases.
- The two liquid-like phases are attributed to a liquid electrolyte and solvated amorphous PVDF phase with distinct viscosities.
- Fluorinated BF<sub>4</sub> anion gave less of an indication of presence in both phases.